

Analyzing the Form-Finding of a Large-Span Transversely Stiffened Suspended Cable System: A Method Considering Construction Processes

Junyu Chen¹, Yanfei Wang², Ke Chen³, Shiqing Huang^{1,4*}, Xiaowen Xu^{4*}

¹MOE Key Lab of Disaster Forecast and Control in Engineering, School of Mechanics and Construction Engineering, Jinan University, Guangzhou, China

²China Construction Second Engineering Bureau Second Company, Shenzhen, China

³Department of Civil Engineering, Dazhou Technician College, Dazhou, China

⁴Key Laboratory of Product Packaging and Logistics, Packaging Engineering Institute, College of Packaging Engineering, Jinan University, Zhuhai, China

Email: *xiaowenxu@jnu.edu.cn, *thuangsq@jnu.edu.cn

How to cite this paper: Chen, J.Y., Wang, Y.F., Chen, K., Huang, S.Q. and Xu, X.W. (2024) Analyzing the Form-Finding of a Large-Span Transversely Stiffened Suspended Cable System: A Method Considering Construction Processes. *World Journal of Engineering and Technology*, 12, 229-244. <https://doi.org/10.4236/wjet.2024.122015>

Received: February 3, 2024

Accepted: March 26, 2024

Published: March 29, 2024

Copyright © 2024 by author(s) and Scientific Research Publishing Inc. This work is licensed under the Creative Commons Attribution International License (CC BY 4.0).

<http://creativecommons.org/licenses/by/4.0/>



Open Access

Abstract

The precise control of the shape of transversely stiffened suspended cable systems is crucial. However, existing form-finding methods primarily rely on iterative calculations that treat loads as fixed known conditions. These methods are inefficient and fail to accurately control shape results. In this study, we propose a form-finding method that analyzes the load response of models under different sag and stress levels, taking into account the construction process. To analyze the system, a structural finite element model was established in ANSYS, and geometric nonlinear analysis was conducted using the Newton-Raphson method. The form-finding analysis results demonstrate that the proposed method achieves precise control of shape, with a maximum shape error ranging from 0.33% to 0.98%. Furthermore, the relationships between loads and tension forces are influenced by the deformed shape of the structures, exhibiting significant geometric nonlinear characteristics. Meanwhile, the load response analysis reveals that the stress level of the self-equilibrium state in the transversely stiffened suspended cable system is primarily governed by strength criteria, while shape is predominantly controlled by stiffness criteria. Importantly, by simulating the initial tensioning process as an initial condition, this method solves for a counterweight that satisfies the requirements and achieves a self-equilibrium state with the desired shape. The shape of the self-equilibrium state is precisely controlled by simulating the construction process. Overall, this work presents a new method for analyzing

the form-finding process of large-span transversely stiffened suspended cable system, considering the construction process which was often overlooked in previous studies.

Keywords

Cable Structure, Long-Span Structure, Form-Finding Analysis, Finite Element Simulation, Transverse Cable Stiffening System

1. Introduction

Cable structures are widely utilized in various applications, such as lightweight roof structures [1], bridge structures [2] [3], and radar antenna [4] fields. These structures are favored due to their attractive shape, high strength, light self-weight, and adaptability, making them a popular choice for large-span structures. However, cables have poor shape stability and cannot withstand pressure force or bending moments. As a result, they exhibit significant displacement when there are changes in load distribution, making cable structures less conducive to carrying loads efficiently. To address this issue and improve the performance of cable structures, one approach is to create a transversely stiffened suspended cable system by installing transverse members [5]. This structural system consists of cables, transverse members, counterweight members, and support structures. The transverse members interact with the cables to maintain the structural shape, and tension in the cables, and balance the dead load, resulting in a self-equilibrium state with sufficient stiffness. The addition of transverse members enhances the stability and stiffness of the cables, transfers loads from the transverse members to the cables, and collectively resists wind and temperature loads, thus improving the overall performance of the roof structure [6].

Designing and constructing a transversely stiffened suspended cable system poses challenges due to the unique characteristics of cables. During construction, the shape of the structure and tension distribution undergo significant changes. Until reaching the design configuration, the structure remains unstable and dynamic [7]. Additionally, the nonlinear relationship between cable displacement and strain, as well as the interaction between cable shape and tension [8], further complicate the determination of the self-equilibrium state. Therefore, accurately determining the self-equilibrium state is crucial for various structures that contain flexible members [9], including cable-membrane structures [10], cable networks [11] [12], tensegrity structures [13], and cable domes [14]. This process is known as form-finding analysis. Among various numerical form-finding methods [15] [16] [17], the force density method [18], dynamic relaxation method [19] [20], and nonlinear finite element method [21] [22] are commonly used. Equations are created by discretizing the structure, and a computer program is employed to solve for the self-equilibrium state. However, the force density me-

thod and dynamic relaxation method are more suited for structures dominated by flexible members, as they do not consider the deformation of rigid members, leading to errors in the calculation results. Accurately calculating the deformation of rigid members requires considering the material properties of these members during the form-finding process, which can be achieved through nonlinear finite element methods [23].

The transversely stiffened suspended cable system consists of both rigid and flexible members. The rigid members are fixed according to the building scheme [24], while the position of the flexible cables varies based on the applied loads [25]. Therefore, it is crucial to adjust counterweights to achieve harmony between the cables and beams. The traditional iterative methods used in nonlinear finite element analysis treat loads as fixed known conditions, resulting in the inability to accurately control the shape of the cables. This discrepancy between the simulation results and the desired effect is unsatisfactory. Moreover, the iterative methods overlook the influence of the construction process on the self-equilibrium state, which forms the basis of load response analysis. Inaccurate modeling with significant errors can lead to serious safety risks. Hence, it is essential to develop a method that considers the construction process and precisely controls the shape of the self-equilibrium state.

In this work, we proposed a form-finding method that considered the construction process and analyzed different sag and stress levels. The method combined the principles of the force density method and nonlinear finite element method, focusing on a transversely stiffened suspended cable system located in the central area of a roof structure project. The structural finite element model was established by ANSYS software, and geometric nonlinear analysis was performed using the Newton-Raphson method. By simulating the initial tensioning process and incorporating the target shape, we determined the necessary counterweight to achieve the self-equilibrium shape and actively adjusted the loads to precisely control the shape. Additionally, we simulated the downward pressing process during construction to efficiently solve the self-equilibrium state of the structure. Furthermore, we conducted load response analysis based on the form-finding results, investigating the effects of counterweight, geometric shape, cable tension force, and other parameters on the structural performance during the form-finding process.

2. Engineering Background

The project is situated in Hangzhou, China. Drawing inspiration from the aesthetics of Chinese traditional culture and blending it with a modern pursuit of flight, the structure's design resembles unfolded wings, as depicted in **Figure 1**. The overall dimensions of the structure encompass a length of 394.8 meters and a width of 155.4 meters, covering a total site area of approximately 61,000 square meters. The upper section of the structure features a steel truss-cable roof comprising south and north extended roofs, along with a central cable area. In



Figure 1. Architectural rendering of this project.

contrast, the lower part of the structure comprises eight buildings, with the inner buildings firmly connected to the upper portion while allowing movement on the outer side through sliding articulations.

The central cable area of the structure adopts a transversely stiffened suspended cable system, with a longitudinal span of 109.2 meters. Along the longitudinal direction, there are 18 cables supported by side trusses arranged in parallel on both sides. The spacing between the cables is 8.4 meters, while the distance between the cables and side trusses is 6.3 meters. In the transverse direction, there are 25 beams and counterweights spanning 155.4 meters. The spacing between the beams varies from 3.9 to 4.2 meters, and there is a distance of 4.95 meters between the beams and the extended roof on both sides. The cables and beams are arranged perpendicular to each other, forming a net-like structure. The cables are connected to the extended roof through articulations at both ends, while the beams are rigidly connected to the side trusses on both sides. This arrangement ensures the self-equilibrium of the structural shape, cable tension, and constant load, resulting in a distinctive concave curved building shape.

3. Form-Finding Method Analysis

The objective of the form-finding analysis is to determine the self-equilibrium state of the structure upon completion of construction. The solution process involves several steps, including modeling, solving for the self-equilibrium state, and verifying the results. The modeling phase entails determining the structural topology, support conditions, loading conditions, materials of the members, section dimensions, geometric shape, and tension distribution. These inputs are used to establish the equilibrium equations. However, since the tension distribution is interrelated with the geometric configuration, an initial value set through estimation is often insufficient to achieve the desired self-equilibrium state. To solve for equilibrium, one criterion is selected as the controlling factor, and the other variables are calculated using the equilibrium equations. The equations are presented below:

$$[K] \cdot U = P \quad (1)$$

$$[K] = [K]^G + [K]^E \quad (2)$$

The stiffness matrix $[K]$ is composed of two parts: the geometric stiffness matrix $[K]^G$ and the linear elasticity stiffness matrix $[K]^E$. The former is related to cable tension, while the latter is connected to sections. The column vector of nodal displacements is represented as U , while the column vector of nodal loads is denoted as P .

Taking force-finding analysis as an example, the calculation of the self-equilibrium state involves controlling the shape of the cables. The process begins by calculating the unbalanced forces at the nodes and iteratively adjusting the cable tensions until the displacements of all nodes are within a specified limit. Since the shape of cable structures is influenced by loads, precise control of the shape requires solving for both tension distribution and counterweights through form-finding analysis. In this case, any variation in either parameter can affect the node displacements. When using iterations alone, it becomes challenging to determine the cause of unbalanced displacements and effectively adjust parameters to achieve self-equilibrium. To address this, the construction process is taken into consideration in this study. By simulating the structure's construction, the counterweights are solved first, followed by controlling the convergence of the structural shape towards the self-equilibrium shape. This approach provides a way to solve for the self-equilibrium state of the structure.

3.1. Construction Steps and Flow of Form-Finding

The construction of a transversely stiffened suspended cable system can be seen as a cumulative installation process involving cables and beams. During construction, the structure is initially constructed by tensioning and anchoring the cables. Subsequently, the cables are pressed downward using beams. This construction process can be divided into two stages: the initial tensioning process and the pressing downward process. In the initial tensioning process, the structure is in a state where only one cable is present, and the cables are loaded solely by self-weight. This loading can be controlled by the target initial tension force T_0 . During the pressing downward process, the displacement of the cables is induced by placing beams on top of them. This process modifies both the shape and tension of the cables. The structure achieves balance through the use of counterweights, with the desired shape being the target at this stage. The self-equilibrium state model of the cable is depicted in **Figure 2**, with the dashed lines indicating the positions of the cables during the initial tensioning process. The loads can be adjusted by utilizing the counterweights.

The construction process revealed that the self-equilibrium state of the transversely stiffened suspended cable system is determined by the initial state of the cables and the pressing downward process. As a result, the solution process for determining the self-equilibrium state in form-finding analysis is divided into

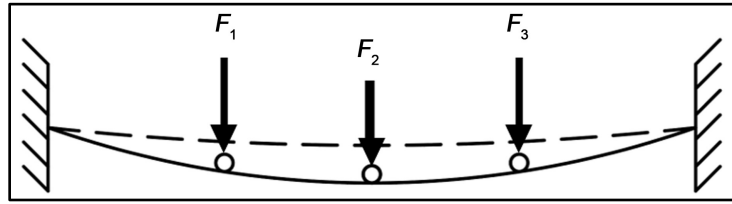


Figure 2. Self-equilibrium state model of the cable.

two stages: the initial state and the construction process for simulation. The flow of the form-finding method is summarized in **Figure 3**.

3.2. Initial State Analysis

The form-finding calculations are based on the following assumptions: The cables are assumed to be ideally flexible, meaning they cannot resist bending moments and pressure. The working state of the cables follows Hooke's law. All loads are concentrated at nodes, and cable segments do not resist loads.

In the initial state analysis, the structure's beams have not been installed, and the cables are fully flexible. The initial state can be calculated using the force density method [18] with the initial tension force T_0 . The equations for this calculation are represented as follows in Equation (3):

$$\begin{aligned} [C]^T \cdot [Q_0] \cdot [C] \cdot X_0 &= P_{x0} \\ [C]^T \cdot [Q_0] \cdot [C] \cdot Y_0 &= P_{y0} \\ [C]^T \cdot [Q_0] \cdot [C] \cdot Z_0 &= P_{z0} \end{aligned} \quad (3)$$

where $[C]$ is topology matrix; $[Q_0]$ is the force density matrix associated with the initial tension force T_0 . P_{x0} , P_{y0} and P_{z0} are nodal load vectors, which are calculated based on the self-weight of the structure. X_0 , Y_0 and Z_0 are node coordinate vectors, which are solved using these equations. This method utilizes force density as a control parameter and mathematically calculates the coordinates of nodes such that the total force at the nodes approaches zero.

3.3. Construction Process Analysis

During the analysis of the construction process, beams and counterweights are placed on the cables to build up tension, which alters the tension distribution and shape of the cables. This process is repeated multiple times until all components are installed and a self-equilibrium state is reached. However, since the force density method does not consider material properties, Equation (3) cannot account for the variation in cable length caused by the loads. Therefore, the non-linear finite element method [21] [22] is employed in this process. When the equilibrium state of the i^{th} iteration is known, the $(i+1)^{\text{th}}$ equilibrium state can be calculated using Equation (4):

$$[K_i] \cdot U_{i+1} = P_{i+1} - P_i + R \quad (4)$$

Here, R represents the residual caused by the geometric nonlinear effect. The

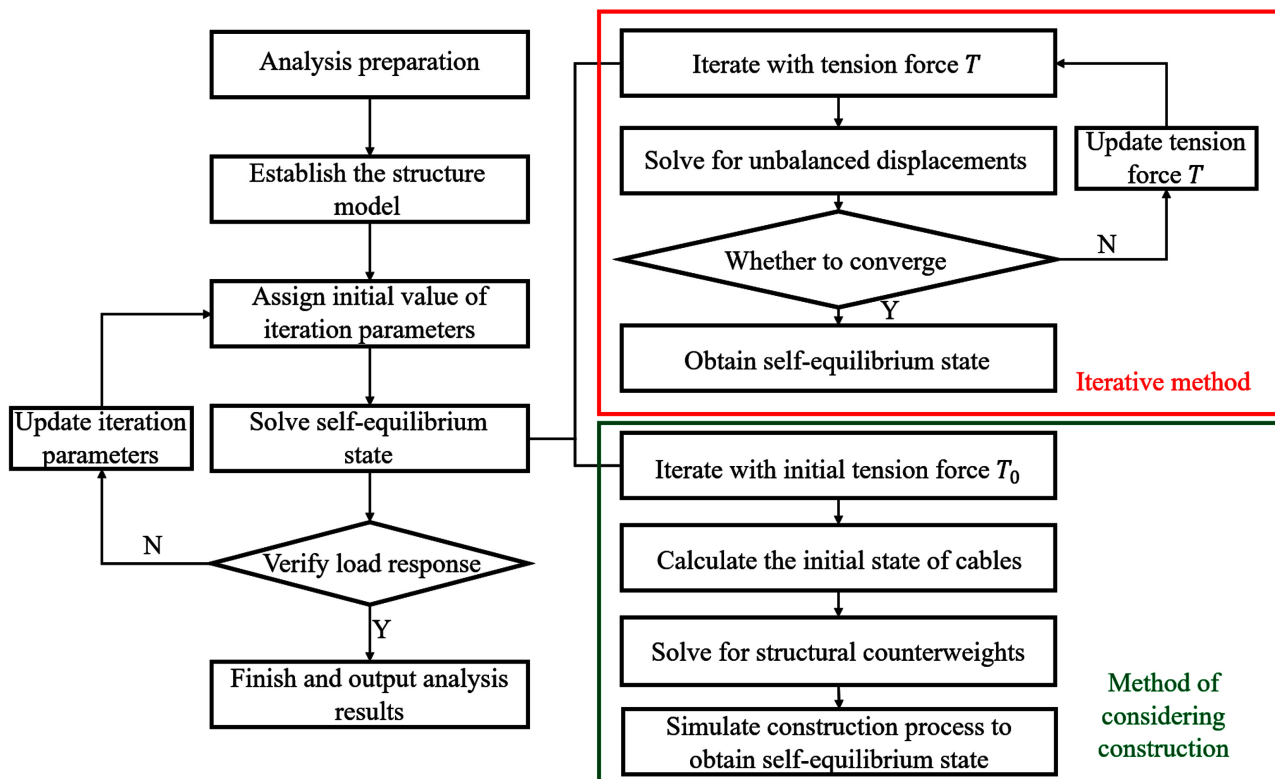


Figure 3. Flowchart of form-finding calculation.

shape of the self-equilibrium state is determined by the building scheme, and the initial state is obtained from Equation (3). Setting the self-equilibrium state as the s^{th} equilibrium state, the total displacement of nodes $U_{x,s}$, $U_{y,s}$ and $U_{z,s}$ can be expressed as follows:

$$\begin{aligned} U_{x,s} &= X_s - X_0 \\ U_{y,s} &= Y_s - Y_0 \\ U_{z,s} &= Z_s - Z_0 \end{aligned} \quad (5)$$

Considering the total displacement of nodes and Equation (4), the column vector of nodal loads P_s can be calculated as the sum of nodal loads from the initial state to the s^{th} equilibrium state:

$$P_s = \sum_{i=0}^{s-1} [K_i] \cdot U_{i+1} + P_0 + R \quad (6)$$

Equation (6) is solved using the Newton-Raphson method, with a convergence criterion determined as follows (in kN):

$$R < 0.005 \quad (7)$$

The nodal loads P_s obtained from Equation (6) represent the loads on the cable-beam connections. However, due to differences in the stiffness of the supporting structure, the load values of nodes on the same beam may vary, making it challenging to achieve during construction. To address this, the actual counterweight P'_s on beams is taken as the average value of all nodes on the beam.

The total loads remain consistent with the results obtained from Equation (6). The self-equilibrium state calculated from Equation (4) using P'_s generally aligns with the desired target shape.

3.4. Element Type and Section Properties

The structural model is created using the general finite element software ANSYS (version 19.2). The form-finding method is implemented using the ANSYS parametric design language (APDL). The model consists of an upper steel cable roof and lower support structures in the central zone. The connection between the lower support structures on both sides is a sliding hinge support. The model is illustrated in Figure 4, and the element types for each component are presented in Table 1.

The extended roof trusses comprise various I-beam, square, and round steel sections of different sizes. The lower supporting structure is a concrete frame-shear wall structure, which includes beams, columns, and walls of different sections and sizes. The cable section has a diameter of 113 mm, equivalent to two 80 mm diameter circular solid sections made of galvanized stainless steel. The transverse beam is a hollow circular steel pipe with a section measuring 245 mm OD and 14 mm thickness. It is constructed from Q355B mild steel.

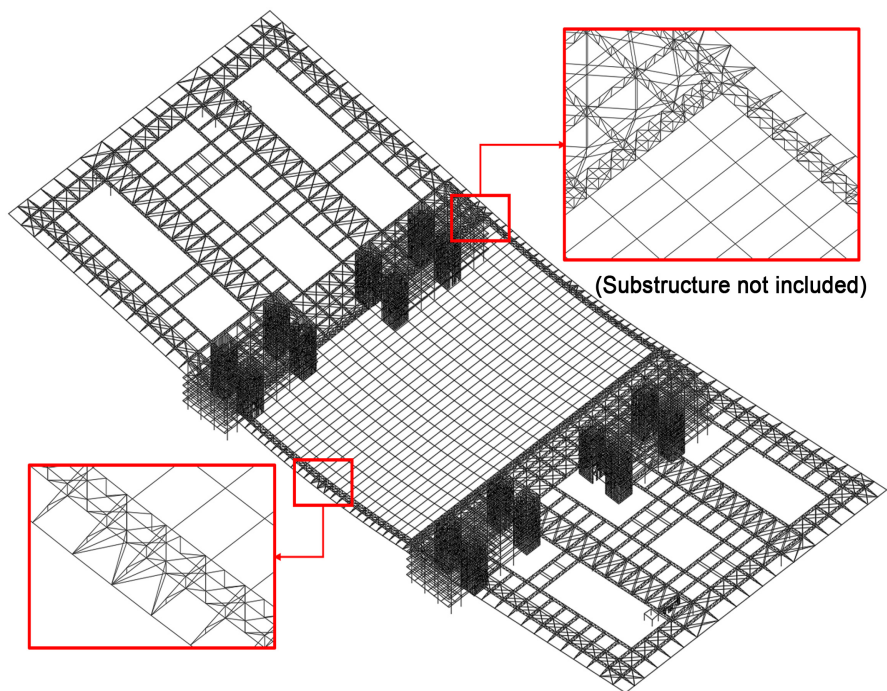


Figure 4. Finite element model.

Table 1. Element types of components.

Components	Truss	Cable	Beam	Support	Wall
Element type	Link 8	Link 10	Beam 44	Link 8	Shell 63

3.5. Simulation Steps for Form-Finding

The simulation process is divided into several steps, as illustrated in **Figure 5**.

Step 1 involves analyzing the initial installation to determine the shape of the single cable. Element birth and death technology is applied to simulate only the cables, and the model is updated based on the calculation results.

Step 2 simulates the installation of both the cables and the support structure using element birth and death technology. The shape of the cable obtained from Step 1 is used, and initial strain is given to the cable elements.

Step 3 involves solving for the counterweight by forcing the cable to deform to the target shape through displacement loading. The constraint reaction force is then read to calculate the counterweight. Upon completion of the calculation, the constraints are released, and the model is restored to the state of Step 2.

Step 4 is the construction analysis, during which beams are gradually installed according to the calculated counterweight and connected with the side trusses. The beam installation order is from both sides towards the center.

Step 5 completes the form-finding analysis after all beams are installed. At this point, the structure's self-equilibrium shape is largely consistent with the target shape.

4. Results

4.1. Form-Finding Results

The form-finding analysis was conducted for a total of 16 models, considering four types of mid-span drops (3.5 m, 5.46 m, 7.28 m, and 10.92 m) and four types of maximum stress levels of the cables (20%, 40%, 60%, and 80%). The results of these analyses are presented in **Table 2**. The data in **Table 2** demonstrates that the maximum shape error for each model falls within the range of

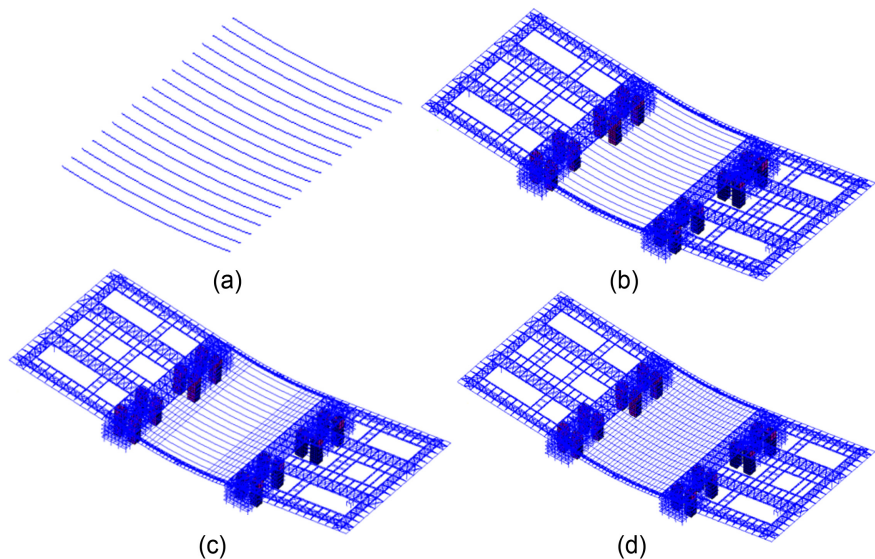


Figure 5. Simulation steps for form-finding: (a) step 1, (b) step 2, step 3, (c) step 4 and (d) step 5.

Table 2. The results of form-finding analysis.

Mid-span sag	Maximum stress level	Initial tension	C.C.	Maximum shape error	Mid-span sag	Maximum stress level	Initial tension	C.C.	Maximum shape error
3.5 m	20%	360.50 kN	0.17	0.72%	7.28 m	20%	166.15 kN	1.01	0.35%
3.5 m	40%	416.00 kN	1.00	0.68%	7.28 m	40%	170.81 kN	2.63	0.53%
3.5 m	60%	500.00 kN	1.79	0.81%	7.28 m	60%	175.80 kN	4.23	0.69%
3.5 m	80%	652.00 kN	2.59	0.98%	7.28 m	80%	181.35 kN	5.82	0.86%
5.46 m	20%	222.50 kN	0.63	0.39%	10.92 m	20%	112.73 kN	1.65	0.33%
5.46 m	40%	234.50 kN	1.88	0.51%	10.92 m	40%	114.15 kN	3.96	0.53%
5.46 m	60%	248.20 kN	3.11	0.66%	10.92 m	60%	115.63 kN	6.27	0.72%
5.46 m	80%	264.00 kN	4.32	0.80%	10.92 m	80%	117.14 kN	8.55	0.91%

Note: The mid-span sag refers to the sag in the mid-span of cables in a self-equilibrium state. The maximum stress level is the ratio of the maximum stress to the design strength of the cables in the self-equilibrium state. Initial tension represents the tension force of cables in the initial state analysis. C.C. denotes the coefficient of counterweight, which is the ratio of the sum of the counterweight obtained from form-finding. The maximum shape error is the ratio of the maximum error to the target shape.

0.33% to 0.98%. This indicates that the method employed accurately controls the self-equilibrium shape. When comparing models with the same mid-span sag, it is observed that increasing the initial tension results in a higher coefficient of counterweight (C.C.) and an elevated maximum stress level. Since the initial tension primarily affects the cable shape in the initial state, the C.C. is derived from the disparity between the self-equilibrium state and the initial state. An augmentation in the initial tension leads to a corresponding increase in the C.C., which subsequently amplifies the maximum stress level. Furthermore, for every 20% increment in the maximum stress level, the C.C. for mid-span drops of 3.5 m, 5.46 m, 7.28 m, and 10.92 m increased approximately by 0.8, 1.2, 1.6, and 2.3, respectively. This implies that the relationship between the loads and stress in cable structures is influenced by the self-equilibrium shape of the structure, exhibiting pronounced geometric nonlinearity characteristics.

4.2. Load Response Results

The results of the form-finding analysis must be verified to ensure that the structure meets safety requirements. In accordance with Article 3.2.13 of the Technical Specification for Cable Structures (JGJ257-2012), the ratio of maximum deflection to span for transversely stiffened suspended cable systems should not exceed 1/250. The design strength of cables typically ranges from 0.4 to 0.5 times the standard strength. Therefore, in compliance with these standards, the maximum deflection and design strength selected for this study were 436.8 mm and 435.6 MPa, respectively.

It is important to note that the results of load response can be calculated using load combinations based on the actual engineering situation, with load values listed in GB 50009-2012. Displacement response is calculated using nominal combinations to simulate the limit state of normal use, while stress response is

calculated using fundamental combinations to simulate the limit state of load-bearing capacity. **Table 3** provides the control load combinations for displacement response. It is explicitly stated that the maximum upward displacement is controlled by wind load and temperature load, while the maximum downward displacement is controlled by live load and temperature load. The displacement response of the structure is primarily influenced by temperature loads. Since the value of the live load is greater than the value of the wind load, the displacement downward is greater than the displacement upward.

Furthermore, we conducted calculations for the displacement response, and the results are presented in **Table 4**. The model names indicate the mid-span sag and stress level of each model, for example, the 3.5 m-20 model has a mid-span sag of 3.5 m and a stress level of 20%. As the load combinations involve two directions, the displacement response of the structure also includes both upward and downward movements, which should be within the limit of 436.8 mm. As shown in **Table 4**, increasing the stress level of the model can reduce the displacement response, indicating that enhancing the geometric stiffness of the cables improves deformation resistance. Additionally, increasing the mid-span sag

Table 3. Control load combinations of displacement response.

Number	Load combination	Number	Load combination
6	1.0DL + 1.0ADL + 1.0TLDN	16	1.0DL + 1.0ADL + 0.6WLUP + 1.0TLDN
10	1.0DL + 1.0ADL + 0.7LL + 1.0TLUP	17	1.0DL + 1.0ADL + 0.6WLDN + 1.0TLUP

Note: The dead load (DL) is determined based on material density. The additional dead load (ADL) represents the counterweight that is determined through form-finding analysis. The live load (LL) is determined for a non-accessible roof with a value of 0.5 kN/m². Wind load (WL) is determined based on the wind tunnel test report, considering the most unfavorable case envelope value with a range of ± 0.12 kN/m². Temperature load (TL) is determined based on the local environment, calculated through the closing temperature, maximum temperature, and minimum temperature with values of +33°C and -29°C. TLUP and TLDN indicate an increase or decrease in temperature load, while WLUP and WLDN represent upward and downward wind loads.

Table 4. The results obtained from displacement response.

Model name	Maximum displacement (upward/mm)	Maximum displacement (downward/mm)	Model name	Maximum displacement (upward/mm)	Maximum displacement (downward/mm)
3.5m-20	-432.35	447.69	7.28m-20	-196.55	207.72
3.5m-40	-358.16	418.05	7.28m-40	-175.73	191.21
3.5m-60	-310.78	386.19	7.28m-60	-165.99	187.05
3.5m-80	-276.05	356.41	7.28m-80	-158.82	184.83
5.46m-20	-260.35	269.72	10.92m-20	-139.10	146.24
5.46m-40	-231.86	258.32	10.92m-40	-122.77	133.09
5.46m-60	-215.05	252.76	10.92m-60	-115.96	126.77
5.46m-80	-201.45	244.62	10.92m-80	-112.47	123.40

can also reduce the displacement response, implying a reduction in the ratio of displacement change caused by axial deformation of the cables.

Next, we performed calculations for the stress response. The control load combination for stress response is listed in **Table 5**, and the results are shown in **Table 6**. As displayed in **Table 5**, the maximum stress is generated by dead load, live load, and wind load. The maximum stress is controlled by dead load and live load, while the minimum stress level is controlled and generated by wind load and temperature load. Since the load combinations involve two directions, the stress response of the structure includes both maximum and minimum stress levels. The maximum stress level should be less than 100%, and the minimum stress level should be higher than the stress level under dead load, which is approximately 5% to 15%. As depicted in **Table 6**, for the 20% and 40% stress level models, increasing the mid-span sag can reduce stress response. However, for the 60% and 80% stress level models, the increase in mid-span sag has a lesser effect on stress response. This trend is influenced by two factors. Firstly, an increase in mid-span sag leads to an increase in counterweight, resulting in a greater stress response. Secondly, the relationship between load and stress response is affected by geometric nonlinearities. With an increase in mid-span sag, the ratio of load to stress response is reduced, thereby decreasing stress response. The stress level of the model impacts the range between maximum and minimum stress response. Therefore, adjusting the model stress level can satisfy the demand for both maximum and minimum stress response and fully utilize the cables' capabilities.

Table 5. Control load combinations for stress response.

Number	Load combination	Number	Load combination
10	1.0DL + 1.0ADL + 1.5WLUP + 0.9TLUP	20	1.3DL + 1.3ADL + 1.5LL + 0.9WLDN
11	1.0DL + 1.0ADL + 0.9WLUP + 1.5TLUP	21	1.35DL + 1.35ADL + 1.05LL

Table 6. The results obtained from stress response.

Model name	Maximum stress level	Minimum stress level	Model name	Maximum stress level	Minimum stress level
3.5m-20	48.98%	8.35%	7.28m-20	40.17%	13.63%
3.5m-40	70.64%	29.39%	7.28m-40	65.29%	33.20%
3.5m-60	92.27%	50.26%	7.28m-60	89.83%	52.46%
3.5m-80	113.98%	70.89%	7.28m-80	114.6%	72.12%
5.46m-20	43.61%	12.31%	10.92m-20	36.28%	14.69%
5.46m-40	67.61%	32.19%	10.92m-40	61.80%	33.09%
5.46m-60	90.94%	51.74%	10.92m-60	88.14%	52.15%
5.46m-80	114.32%	71.51%	10.92m-80	113.15%	70.32%

5. Discussion

The form-finding process for transversely stiffened suspended cable systems is a crucial design process. It involves determining the section, shape, tension distribution, and counterweight of the system. The complex relationships between these parameters make it challenging for designers to adjust them based on the structural response. The effectiveness of parameter adjustments largely depends on the designer's experience. Therefore, it is important to establish the range of unknown parameters and improve the efficiency of loop parameter control through load response analysis.

Structural verification encompasses strength, stiffness, and stability. The cable structure primarily experiences tensile forces and is equipped with transverse members to ensure good stability performance. Strength and stiffness criteria are verified by examining load responses under different combinations of loads. These load combinations are determined based on the structure's function, arrangement, and working environment. Consequently, it becomes necessary to adjust the results obtained from the form-finding analysis using load responses.

Strength verification includes assessing cable stress, beam stress, and the bearing capacity of the support. The bearing capacity of the support determines the cable's maximum tension and section size. Beam stress is influenced by the counterweight, similar to that of a multi-span continuous beam. The stress response of the cable comprises three components: self-weight, construction tension, and load response. Taking the 3.5 m drap model as an example (as shown in **Figure 6**), the stress composition of different models reveals minimal variation in the self-weight and load response parts, whereas the construction tension

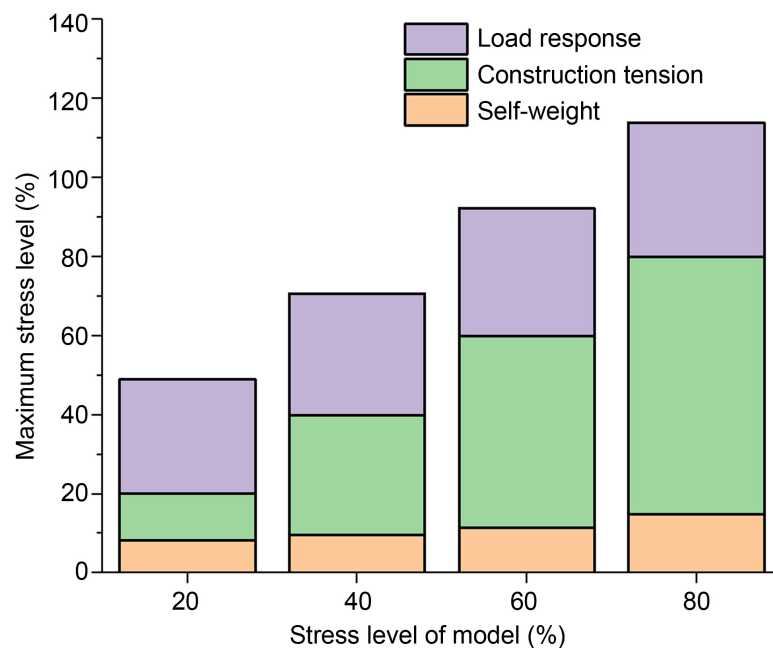


Figure 6. The plot of maximum stress level versus stress level of sample 3.5 m model.

part shows significant differences. The cable's self-weight contributes to approximately 10% of the stress level, while the stress response under load increases 2 to 4 times more than the decrease. Consequently, during form-finding analysis, it is suitable to control the stress level of the model within the range of 28% to 40% to optimize cable performance.

Stiffness criteria are verified by examining displacement responses. Due to geometric nonlinearities, the relationship between displacement and cable strain is nonlinear and influenced by the shape of the cable. Cable strains are partly generated by changes in cable stress due to applied loads. By increasing the linear elastic stiffness through section area or enhancing geometric stiffness by raising the model's stress level, the stress variation can be reduced, thereby minimizing displacement response. The other portion of cable strain is caused by temperature load, which is determined by the local climate and cannot be altered. Consequently, increasing cable section, stress level, and mid-span sag can help reduce displacement response. If enhancing the cable section and stress level to their limits still fails to meet the structural stiffness requirements, it indicates an unreasonable structural shape, necessitating modifications to the shape design.

6. Conclusion

In this study, we have developed a form-finding method for transversely stiffened suspended cable systems that takes the construction process into account. The validity and accuracy of the method have been verified through an actual project. The results of the form-finding analysis demonstrate that the maximum shape error for each model falls within the range of 0.33% to 0.98%. This indicates that the method can effectively control the self-equilibrium shape with high accuracy. Increasing the initial tension leads to a corresponding increase in the counterweight, resulting in higher maximum stress levels. The relationship between loads and stress is influenced by the structure's shape, and the presence of geometric nonlinearities is evident. Load response analysis reveals that the cable section and cable tension are primarily governed by strength criteria. It is recommended to maintain the self-equilibrium stress level within the range of 28% to 40% in order to optimize cable performance. It also demonstrates that shape control is primarily influenced by stiffness criteria. Increasing the cable section, cable tension, and mid-span sag all contribute to reducing displacement response. Overall, the method that takes the actual construction process into account has shown great potential for real-life applications.

CRedit Authorship Contribution Statement

Junyu Chen: Investigation, Software, Methodology. Yanfei Wang & Ke Chen: Resources. Shiqing Huang & Xiaowen Xu: Conceptualization, Validation, Formal analysis, Resources, Supervision, Writing-original draft, Writing-review & editing, Funding acquisition, Project-administration.

Data Availability

Data will be made available on request.

Declaration of Competing Interest

The authors declare that they have no known competing financial interests or personal relationships that could have appeared to influence the work reported in this paper.

References

- [1] Xue, S., Li, X. and Liu, Y. (2022) Advanced Form Finding of Cable Roof Structures Integral with Supporting Frames: Numerical Methods and Case Studies. *Journal of Building Engineering*, **60**, Article ID: 105204. <https://doi.org/10.1016/j.jobbe.2022.105204>
- [2] Tian, G.-M. and Zhang, W.-M. (2023) A Semi-Analytical Form-Finding Method of the 3D Curved Cable Considering Its Flexural and Torsional Stiffnesses in Suspension Bridges. *Applied Mathematical Modelling*, **124**, 806-839. <https://doi.org/10.1016/j.apm.2023.08.027>
- [3] Chai, S.-B., Wu, Q. and Wang, X.-L. (2023) Deformation and Force Characteristics of Double-Cable Suspension Bridges. *Structures*, **54**, 1705-1716. <https://doi.org/10.1016/j.istruc.2023.05.102>
- [4] Nie, R., He, B., Hodges, D.H., *et al.* (2019) Integrated Form Finding Method for Mesh Reflector Antennas Considering the Flexible Truss and Hinges. *Aerospace Science and Technology*, **84**, 926-937. <https://doi.org/10.1016/j.ast.2018.11.034>
- [5] Ye, J., Feng, R.-Q., Zhao, X., *et al.* (2012) A Form-Finding Method of Beam String Structures—Offload by Steps Method. *International Journal of Steel Structures*, **12**, 267-283. <https://doi.org/10.1007/s13296-012-2010-1>
- [6] Krishnan, S. (2020) Cable-Stayed Columns and Their Applications in Building Structures. *Journal of Building Engineering*, **27**, Article ID: 100984. <https://doi.org/10.1016/j.jobbe.2019.100984>
- [7] Chen, L.-M. and Dong, S.-L. (2013) Optimal Prestress Design and Construction Technique of Cable-Strut Tension Structures with Multi-Overall Selfstress Modes. *Advances in Structural Engineering*, **16**, 1633-1644. <https://doi.org/10.1260/1369-4332.16.10.1633>
- [8] Liu, H., Zhang, W., Yuan, H., *et al.* (2016) Modified Double-Control Form-Finding Analysis for Suspendomes Considering the Construction Process and the Friction of Cable-Strut Joints. *Engineering Structures*, **120**, 75-81. <https://doi.org/10.1016/j.engstruct.2016.04.023>
- [9] Zhao, Y., Guo, J., Jiang, Z., *et al.* (2022) Control Method for Determining Feasible Pre-Stresses of Cable-Struts Structure. *Thin-Walled Structures*, **174**, Article ID: 109159. <https://doi.org/10.1016/j.tws.2022.109159>
- [10] Harber, R.B. (1982) Initial Equilibrium Solution Methods for Cable Reinforced Membranes Part I—Formulations. *Computer Methods in Applied Mechanics & Engineering*, **30**, 263-284. [https://doi.org/10.1016/0045-7825\(82\)90080-9](https://doi.org/10.1016/0045-7825(82)90080-9)
- [11] Nie, R., He, B., Hodges, D.H., *et al.* (2019) Form Finding and Design Optimization of Cable Network Structures with Flexible Frames. *Computers & Structures*, **220**, 81-91. <https://doi.org/10.1016/j.compstruc.2019.05.004>
- [12] Li, X., Xue, S. and Liu, Y. (2022) A Novel Form Finding Method for Minimum Sur-

- face of Cable Net. *Journal of Building Engineering*, **48**, Article ID: 103939. <https://doi.org/10.1016/j.jobbe.2021.103939>
- [13] Cai, J., Wang, X., Deng, X., *et al.* (2018) Form-Finding Method for Multi-Mode Tensegrity Structures Using Extended Force Density Method by Grouping Elements. *Composite Structures*, **187**, 1-9. <https://doi.org/10.1016/j.compstruct.2017.12.010>
- [14] Feng, Y., Yuan, X. and Samy, A. (2022) Analysis of New Wave-Curved Tensegrity Dome. *Engineering Structures*, **250**, Article ID: 113408. <https://doi.org/10.1016/j.engstruct.2021.113408>
- [15] Lewis, W.J. (2008) Computational Form-Finding Methods for Fabric Structures. *Engineering & Computational Mechanics*, **161**, 139-149. <https://doi.org/10.1680/eacm.2008.161.3.139>
- [16] Pellegrino, S. (1993) Structural Computations with the Singular Value Decomposition of the Equilibrium Matrix. *International Journal of Solids and Structures*, **30**, 3025-3035. [https://doi.org/10.1016/0020-7683\(93\)90210-X](https://doi.org/10.1016/0020-7683(93)90210-X)
- [17] Veenendaal, D. and Block, P. (2012) An Overview and Comparison of Structural Form Finding Methods for General Networks. *International Journal of Solids and Structures*, **49**, 3741-3753. <https://doi.org/10.1016/j.ijsolstr.2012.08.008>
- [18] Schek, H.J. (1974) The Force Density Method for Form Finding and Computation of General Networks. *Computer Methods in Applied Mechanics and Engineering*, **3**, 115-134. [https://doi.org/10.1016/0045-7825\(74\)90045-0](https://doi.org/10.1016/0045-7825(74)90045-0)
- [19] Lewis, W.J., Jones, M.S. and Rushton, K.R. (1984) Dynamic Relaxation Analysis of the Non-Linear Static Response of Pretensioned Cable Roofs. *Computers & Structures*, **18**, 989-997. [https://doi.org/10.1016/0045-7949\(84\)90142-1](https://doi.org/10.1016/0045-7949(84)90142-1)
- [20] Barnes, M.R. (1988) Form-Finding and Analysis of Prestressed Nets and Membranes. *Computers & Structures*, **30**, 685-695. [https://doi.org/10.1016/0045-7949\(88\)90304-5](https://doi.org/10.1016/0045-7949(88)90304-5)
- [21] Argyris, J.H., Angelopoulos, T. and Bichat, B. (1974) A General Method for the Shape Finding of Lightweight Tension Structures. *Computer Methods in Applied Mechanics and Engineering*, **3**, 135-149. [https://doi.org/10.1016/0045-7825\(74\)90046-2](https://doi.org/10.1016/0045-7825(74)90046-2)
- [22] Tabarrok, B. and Qin, Z. (1992) Nonlinear Analysis of Tension Structures. *Computers & Structures*, **45**, 973-984. [https://doi.org/10.1016/0045-7949\(92\)90056-6](https://doi.org/10.1016/0045-7949(92)90056-6)
- [23] Talvik, I. (2001) Finite Element Modelling of Cable Networks with Flexible Supports. *Computers & Structures*, **79**, 2443-2450. [https://doi.org/10.1016/S0045-7949\(01\)00077-3](https://doi.org/10.1016/S0045-7949(01)00077-3)
- [24] Dong, W., Stafford, P.J. and Ruiz-Teran, A.M. (2019) Inverse Form-Finding for Tensegrity Structures. *Computers & Structures*, **215**, 27-42. <https://doi.org/10.1016/j.compstruc.2019.01.009>
- [25] Zhang, Q., Wang, X., Cai, J., *et al.* (2021) Prestress Design for Cable-Strut Structures by Grouping Elements. *Engineering Structures*, **244**, Article ID: 112010. <https://doi.org/10.1016/j.engstruct.2021.112010>